Systems/Circuits

Descending Dopaminergic Inputs to Reticulospinal Neurons Promote Locomotor Movements

Dimitri Ryczko,[1,2,3] Swantje Grätsch,[1] Michael H. Alpert,[4] Jackson J. Cone,[5] Jacquelin Kasemir,[1] Angelina Ruthe,[1] Philippe-Antoine Beauséjour,[1] François Auclair,[1] Mitchell F. Roitman,[5] Simon Alford,[6] and Réjean Dubuc[1,7]

[1]Department of Neuroscience, Université de Montréal, Montréal, Québec H3C 3J7, Canada, [2]Department of Pharmacology-Physiology, Université de Sherbrooke, Sherbrooke J1H 5N4, Québec Canada, [3]Centre de recherche du CHUS, Sherbrooke, J1H 5N4, Québec, Canada, [4]Department of Biological Sciences, University of Illinois at Chicago, Chicago IL 60607, Illinois, [5]Department of Psychology, University of Illinois at Chicago, Chicago IL 60607, Illinois, [6]Department of Anatomy and Cell Biology, University of Illinois at Chicago, Chicago IL 60612-7308, Illinois, and [7]Groupe de Recherche en Activité Physique Adaptée, Department of Exercise Science, Université du Québec à Montréal, Montréal, Québec H3C 3P8, Canada

Meso-diencephalic dopaminergic neurons are known to modulate locomotor behaviors through their ascending projections to the basal ganglia, which in turn project to the mesencephalic locomotor region, known to control locomotion in vertebrates. In addition to their ascending projections, dopaminergic neurons were found to increase locomotor movements through direct descending projections to the mesencephalic locomotor region and spinal cord. Intriguingly, fibers expressing tyrosine hydroxylase (TH), the rate-limiting enzyme of dopamine synthesis, were also observed around reticulospinal neurons of lampreys. We now examined the origin and the role of this innervation. Using immunofluorescence and tracing experiments, we found that fibers positive for dopamine innervate reticulospinal neurons in the four reticular nuclei of lampreys. We identified the dopaminergic source using tracer injections in reticular nuclei, which retrogradely labeled dopaminergic neurons in a caudal diencephalic nucleus (posterior tuberculum [PT]). Using voltammetry in brain preparations isolated *in vitro*, we found that PT stimulation evoked dopamine release in all four reticular nuclei, but not in the spinal cord. In semi-intact preparations where the brain is accessible and the body moves, PT stimulation evoked swimming, and injection of a D_1 receptor antagonist within the middle rhombencephalic reticular nucleus was sufficient to decrease reticulospinal activity and PT-evoked swimming. Our study reveals that dopaminergic neurons have access to command neurons that integrate sensory and descending inputs to activate spinal locomotor neurons. As such, our findings strengthen the idea that dopamine can modulate locomotor behavior both via ascending projections to the basal ganglia and through descending projections to brainstem motor circuits.

Key words: dopamine; lamprey; locomotion; reticulospinal neurons

Significance Statement

Meso-diencephalic dopaminergic neurons play a key role in modulating locomotion by releasing dopamine in the basal ganglia, spinal networks, and the mesencephalic locomotor region, a brainstem region that controls locomotion in a graded fashion. Here, we report in lampreys that dopaminergic neurons release dopamine in the four reticular nuclei where reticulospinal neurons are located. Reticulospinal neurons integrate sensory and descending suprareticular inputs to control spinal interneurons and motoneurons. By directly modulating the activity of reticulospinal neurons, meso-diencephalic dopaminergic neurons control the very last instructions sent by the brain to spinal locomotor circuits. Our study reports on a new direct descending dopaminergic projection to reticulospinal neurons that modulates locomotor behavior.

Received Oct. 9, 2019; revised Sep. 1, 2020; accepted Sep. 24, 2020.

Author contributions: D.R., F.A., and R.D. designed research; D.R., S.G., M.H.A., J.J.C., J.K., A.R., P.-A.B., and F.A. performed research; D.R., S.G., J.J.C., J.K., A.R., P.-A.B., and F.A. analyzed data; D.R. wrote the first draft of the paper; D.R., S.G., M.H.A., J.J.C., P.-A.B., F.A., M.F.R., S.A., and R.D. edited the paper; D.R. and R.D. wrote the paper.

The authors declare no competing financial interests.

This work was supported by the Canadian Institutes of Health Research 15129 to R.D. and 407083 to D.R.; Fonds de la Recherche du Québec-Santé, Groupe de Recherche sur le Système Nerveux Central, GRSNC, 5249 and FRQS Junior 1 Awards 34920 and 36772 to D.R.; National Institutes of Health DA025634 to M.F.R.; Natural Sciences and Engineering Research Council of Canada 217435 to R.D. and RGPIN-2017-05522 and RTI-2019-00628 to D.R.; Canada Foundation for Innovation 39344 to D.R.; Centre de Recherche du Centre Hospitalier Universitaire de Sherbrooke (start-up funding and PAFI); Faculté de médecine et des sciences de la santé (start-up funding), fonds Jean-Luc Mongrain de la fondation du Centre Hospitalier Universitaire de Sherbrooke, and Centre d'Excellence en Neurosciences de l'Université de Sherbrooke to D.R.; and Great Lakes Fishery Commission 54011 and 54021 to R.D. All relevant data are available from the authors. We thank Danielle Veilleux for technical assistance; and Frédéric Bernard for help with the graphics.

Correspondence should be addressed to Dimitri Ryczko at dimitri.ryczko@gmail.com or Réjean Dubuc at rejean.dubuc@gmail.com.

https://doi.org/10.1523/JNEUROSCI.2426-19.2020

Copyright © 2020 the authors

Introduction

Meso-diencephalic dopaminergic (DA) neurons play a key role in locomotor control. Traditionally, they are considered to do so through their ascending projections to the basal ganglia (Carlsson et al., 1958; Poirier and Sourkes, 1965; Sourkes and Poirier, 1965; Kravitz et al., 2010), which in turn project to a brainstem locomotor center (Dubuc, 2009) controlling locomotion, the mesencephalic locomotor region (MLR) (Shik et al., 1966; Garcia-Rill et al., 1987; Sirota et al., 2000; Cabelguen et al., 2003; Roseberry et al., 2016; Caggiano et al., 2018; Josset et al., 2018; for review, see Ryczko and Dubuc, 2013, 2017). The MLR controls locomotion in a graded fashion by sending descending inputs to reticulospinal (RS) neurons, which relay the locomotor command to spinal locomotor circuits (Orlovskiĭ, 1970; Buchanan and Grillner, 1987; Ohta and Grillner, 1989; Sholomenko et al., 1991; Bretzner and Brownstone, 2013; Hagglund et al., 2010; Kinkhabwala et al., 2011; Kimura et al., 2013; Ryczko et al., 2016a).

In addition to their ascending projections, meso-diencephalic DA neurons were recently found to send descending projections that modulate locomotor circuits in the brainstem and spinal cord. In lampreys and salamanders, DA neurons from a meso-diencephalic nucleus (posterior tuberculum [PT]) send descending projections to the MLR where they release dopamine (lamprey: Ryczko et al., 2013, 2017; Perez-Fernandez et al., 2014; salamander: Ryczko et al., 2016c). These descending DA inputs increase the frequency of swimming movements by amplifying glutamatergic inputs to the MLR through D_1 receptors in lampreys (Ryczko et al., 2013, 2017). In rodents, the descending DA innervation of the MLR originates from A8/A9 (Ryczko et al., 2016c) and A13 (Sharma et al., 2018) (for review, see Fougère et al., 2019). Such DA innervation of the MLR is conserved in monkeys (Rolland et al., 2009) and humans (Ryczko et al., 2016c). In addition to these DA projections to the MLR, A11 sends descending DA projections to the ventral spinal cord that increase spontaneous locomotor activity in mammals (Yoshida and Tanaka, 1988; Koblinger et al., 2014, 2018). In zebrafish, dopamine release in the spinal cord increases motoneuron activity in response to visual stimulation (Jha and Thirumalai, 2020; see also van der Zouwen and Ryczko, 2020). Together, these studies uncovered new substrates through which dopamine directly influences locomotor circuits, in addition to the well-established ascending pathways to the basal ganglia (for review, see Kim et al., 2017; Fougère et al., 2019).

Some studies support the idea that the RS system could be a target for DA neuromodulation as well. The RS system is the final common descending pathway (Dubuc et al., 2008). It integrates both descending commands and sensory inputs, and it shapes motor output by sending monosynaptic inputs to spinal interneurons and motoneurons (for review, see Brownstone and Chopek, 2018). In the lamprey spinal cord, dopamine inhibits RS glutamatergic transmission to spinal locomotor circuits through D_2 receptors (Svensson et al., 2003). In the brainstem of teleosts, DA fibers innervate RS cells (Pereda et al., 1992; McLean and Fetcho, 2004). Dopamine application over RS neurons increases synaptic responses evoked by vestibulocochlear nerve stimulation through D_1 receptors in teleosts (Pereda et al., 1992, 1994; Kumar and Faber, 1999). However, the source of DA innervation to RS neurons and its role in locomotor control have not been resolved.

Here, we show in lampreys that DA neurons from the PT project to the four reticular nuclei, that is, mesencephalic reticular nucleus (MRN), and anterior (ARRN), middle (MRRN), and posterior (PRRN) rhombencephalic reticular nuclei, which together contain most RS neurons. We found that PT stimulation evokes dopamine release in all reticular nuclei. PT stimulation evokes swimming movements (Derjean et al., 2010; Gariépy et al., 2012a; Ryczko et al., 2013, 2017), and blockade of D_1 receptors in a single reticular nucleus (the MRRN) was sufficient to decrease local RS activity and locomotor movements. The pathway reported here adds up to the previously reported DA innervation of the MLR, through which locomotion initiation is modulated according to the internal goals of the animal. By acting directly on RS cells, DA inputs can modulate descending inputs shaped by external inputs. Therefore, meso-diencephalic DA neurons modulate the locomotor circuitry at several levels, including the basal ganglia, MLR, RS system, and spinal cord.

Materials and Methods

Ethics statement. The procedures conformed to the guidelines of the Canadian Council on Animal Care and were approved by the animal care and use committees of both the Université de Montréal and the Université du Québec à Montréal. A total of 51 larval sea lampreys (*Petromyzon marinus*) were used. The sex of the animals was not taken into account; therefore, the present study was not biased to one sex. Care was taken to minimize the number of animals used and their suffering.

Semi-intact and isolated brain preparations. The preparations were similar to the ones used in previous studies (Brocard et al., 2010; Derjean et al., 2010; Ryczko et al., 2013, 2017; Juvin et al., 2016; Grätsch et al., 2019). Briefly, larval animals were anesthetized for 8–10 min with tricaine methanesulfonate (MS 222, 200 mg/L, Sigma Millipore) dissolved in a Ringer's solution (in mM as follows: 130 NaCl, 2.1 KCl, 2.6 $CaCl_2$, 1.8 $MgCl_2$, 4.0 HEPES, 4.0 dextrose, and 1.0 $NaHCO_3$, pH 7.4) and then transferred into an oxygenated cold Ringer's solution. The skin and muscles were removed from the rostral part of the animal, the dorsal cranium was opened, and the rostral spinal segments were exposed. A transverse section was made between diencephalon and telencephalon, and the brain tissue rostral to the PT was removed. The ventral cranium was pinned down dorsal side up in the recording chamber. The body was free to move in a chamber monitored with a video camera. To provide access to the PT, a mid-sagittal section was performed dorsally at diencephalon level. One hour was allocated for recovery before the experiments began. For isolated brain preparations, the same dissection was used, but the body was removed.

Electrophysiology and stimulation. For intracellular recordings, sharp glass microelectrodes (90–125 MΩ) filled with 4 M potassium acetate were used. Signals were amplified with an Axoclamp 2A (Molecular Devices) and recorded (sampling rate of 5–10 kHz) through a Digidata 1200 series interface coupled with Clampex 9.0 (Brocard et al., 2010; Ryczko et al., 2013). Only neurons with a membrane potential <-60 mV and held stable for 15 min after impalement were included in the study. To measure the drug effects on spiking activity, 5 trials were recorded for each cell and for each drug condition. For electrical stimulation, glass-coated tungsten microelectrodes (0.7–3.1 MΩ with 10–40 μm exposed tip) connected to a Grass S88 stimulator (Astro Med) coupled with a Grass PSIU6 photoelectric isolation unit for controlling stimulation intensity (Astro Med) were used. The stimulation site was identified based on previous studies (Derjean et al., 2010; Gariépy et al., 2012a; Ryczko et al., 2013, 2017). Electrical stimulation consisted of a train of square pulses (2 ms duration) applied with a frequency of 5 Hz for 10 s. A pause of 3–5 min was made between two trains of stimulation. The stimulation intensity ranged from 3 to 35 μA.

Drug application. Chemicals were purchased from Sigma Millipore and diluted to their final concentration in Ringer's solution. In some experiments, a Ringer's solution containing the D_1 receptor antagonist SCH 23390 (0.5 mM) (Ryczko et al., 2013, 2017) was microinjected in the MLR. In some experiments, a Ringer's solution containing D-glutamate (5 mM) was also microinjected in the PT (Ryczko et al., 2013, 2016a, 2017). The microinjection procedure was as previously described (e.g., Brocard and Dubuc, 2003; Le Ray et al., 2003; Derjean et al., 2010;

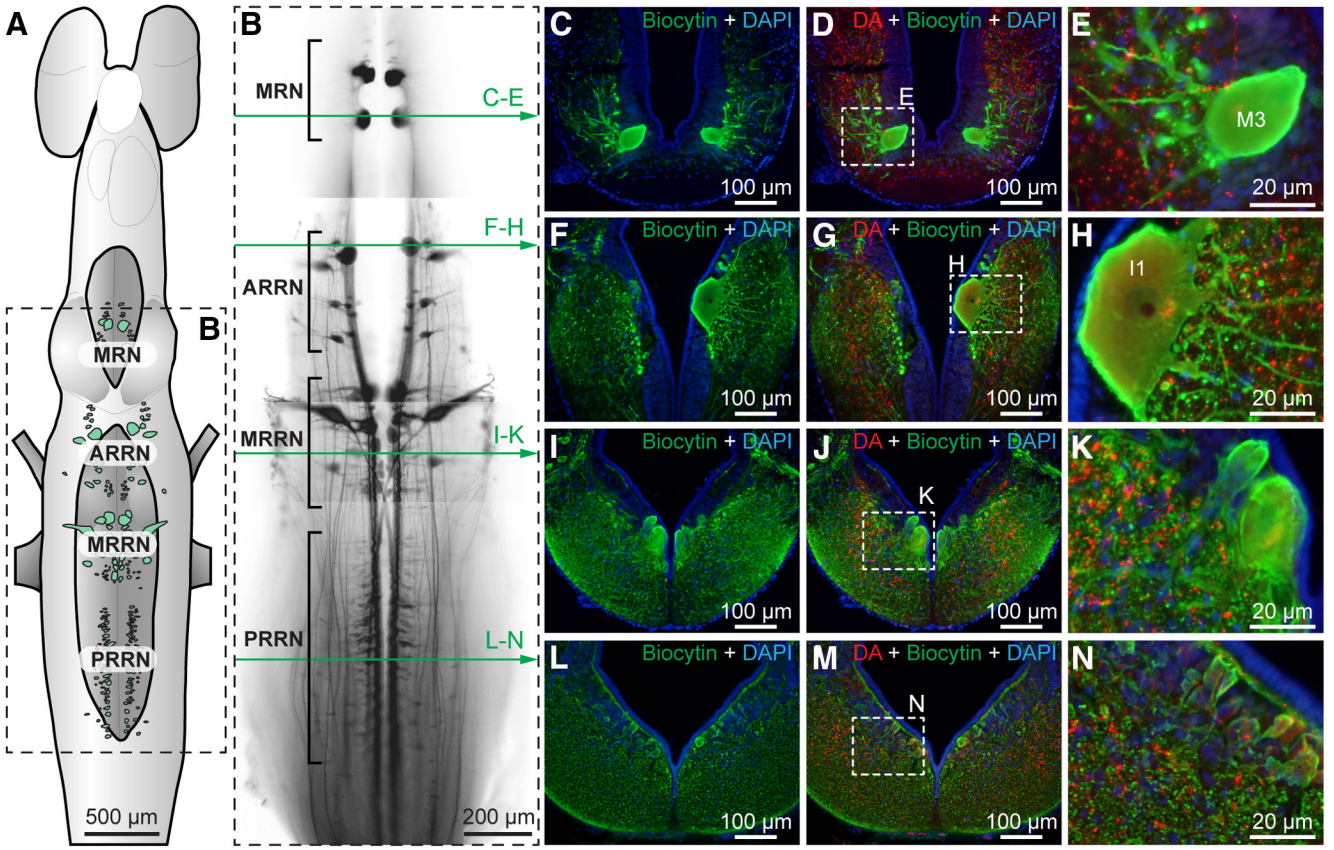

Figure 1. DA-positive innervation of the four reticular nuclei in lampreys. ***A***, Schematic dorsal view of a larval lamprey brain. ***B***, Whole mount of the brainstem illustrating RS cells retrogradely labeled with a tracer (TRDA, black) injected at the level of the second spinal segment. Horizontal green arrows indicate the level of the cross sections shown on the right for each reticular nucleus (photomicrographs in ***C–N***). ***C–N***, DA (red)-containing fibers in close proximity with cell bodies and dendrites of RS neurons in the MRN (***C–E***), ARRN (***F–H***), MRRN (***I–K***), and PRRN (***L–N***). The RS cells were retrogradely labeled by a tracer (biocytin, green) injection at the level of the second spinal segment. ***E***, ***H***, ***K***, ***N***, Magnifications of the dashed rectangles in ***D***, ***G***, ***J***, and ***M***, respectively. ***C–N***, Blue represents DAPI labeling. Data from ***B*** and ***C–N*** were obtained from two different preparations. M3: Mesencephalic Müller cell M3; I1: Isthmic Müller cell I1.

Gariépy et al., 2012a; Ryczko et al., 2013, 2016a,b,c, 2017; Grätsch et al, 2019). The microinjections were done with a glass micropipette (tip diameter of 4-20 µm) using pressure pulses (2.5–15 psi) of variable duration (20-200 ms) applied with a Picospritzer (General Valve). Fast Green was added to the injected solution to monitor the extent of the injection site. The injected volumes were calculated by measuring the diameter of a droplet ejected in air from the tip of the pipette by one pressure pulse and then multiplied by the number of pressure pulses, and the resulting number of moles ejected was calculated (Le Ray et al., 2003; Ryczko et al., 2013, 2016a,b,c, 2017).

Voltammetry. Changes in dopamine concentration were measured using fast-scan cyclic voltammetry with glass-insulated, nafion-coated, carbon-fiber microelectrodes as previously described (Roitman et al., 2008; Ryczko et al., 2013, 2016c). The voltage of the electrode was held at −0.4 V and ramped in a triangular fashion (−0.4 to 1.3 to −0.4 V; 400 V/s; "scan") at 60 Hz during a 30 min equilibration period, during which time no data were collected. During recordings, scans were applied at 10 Hz. Electroactive species within this voltage range oxidize and reduce at different points along the voltage scan and can be identified based on their background-subtracted current by voltage plots (i.e., cyclic voltammogram) (Roitman et al., 2008; Ryczko et al., 2013, 2016c). Dopamine was identified by its traditional oxidation peak (~0.6 V) in lampreys (Ryczko et al., 2013), salamanders (Ryczko et al., 2016c), and rats (Roitman et al., 2008; Sinkala et al., 2012; Ryczko et al., 2016c). Although the dopamine peak can overlap with that of noradrenaline, this is unlikely here because using TH mRNA ISH, no noradrenergic nucleus equivalent to the locus coeruleus was identified in *Petromyzon marinus* (Barreiro-Iglesias et al., 2010). The recording electrode was slowly lowered under visual guidance in the MRN, ARRN, MRRN, or PRRN, which are easily identifiable by the giant RS neurons visible by shining white light from under the preparation (see Fig. 1*A*). An Ag/AgCl reference electrode was placed in the bath. Trains of stimulation were delivered to the PT, and the resultant changes in current at each potential of the electrode were examined. The signals recorded in the lamprey nervous system were compared with that obtained when a solution of dopamine was bath-applied on the voltammetry electrode in a flow cell as previously described (Ryczko et al., 2013, 2016c).

Kinematic analysis. Swimming was monitored with a video camera (Sony HDR-XR200; 30 frames/s) positioned 1 m above the recording chamber. Data were analyzed using custom software (Brocard et al., 2010; Gariépy et al., 2012a; Ryczko et al., 2013, 2017; Juvin et al., 2016; Grätsch et al., 2019). Briefly, equally spaced tracking markers were added digitally offline along the body and monitored over time. Swimming was identified by mechanical waves traveling from head to tail (Sirota et al., 2000; Ryczko et al., 2013, 2017). The frequency of swimming movements, number of locomotor cycles, and locomotor bout duration were quantified using a single couple of markers located in the middle part of the body.

Anatomical tracing and immunofluorescence. Isolated brain preparations were used for these experiments. Biocytin (Sigma-Aldrich) was used for retrograde tracing of PT or RS neurons as previously described (e.g., Gariépy et al., 2012a,b; Ryczko et al., 2013, 2016a,c; Grätsch et al., 2019). First, a pulled glass micropipette was used to perform a lesion at the injection site in the MRN, ARRN, MRRN, PRRN, or MLR. For spinal cord injections, a complete transverse section was made at the level of the second segment. In all cases, crystals of biocytin or Texas Red-conjugated dextran amines (TRDA, 3000 MW, Invitrogen) were immediately placed at the lesion site, allowing the dissolving tracer to be picked up by cut axons. After 10-15 min, the injection site was rinsed thoroughly, and the brain was transferred to a chamber perfused with cold oxygenated

Ringer's solution overnight to allow retrograde transport of the tracer. The injection sites were chosen based on previous studies on RS neurons and on the MLR (e.g., Brocard and Dubuc, 2003; Brocard et al., 2010; Derjean et al., 2010; Ryczko et al., 2013, 2017; Juvin et al., 2016; Grätsch et al., 2019). The next day, the brain was transferred to a fixative solution according to the immunofluorescence procedure to follow.

Individual RS neurons were filled iontophoretically in a brain whole mount. First, sharp microelectrodes were filled with 4 M potassium acetate and 0.5% biocytin (Sigma Millipore), and depolarizing pulses (0.5–1.0 nA, 200 ms duration) were delivered at 1 Hz for 10 min. Then, RS cells were retrogradely labeled after the end of the experiment by applying TRDA on the rostral stump of the transversely cut spinal cord at the level of the second spinal segment. The brain was perfused with cold oxygenated Ringer's solution overnight at 4°C to allow dye transport. Next, the brain was fixed in 4% PFA (Thermo Fisher Scientific) for 24 h at 4°C and transferred into a solution containing AlexaFluor-488 conjugated streptavidin (1:200, Invitrogen) diluted in Triton X-100 (0.5%) and PBS for 24 h. After reaction with biocytin, the tissue was dehydrated by successive immersions (5 min each) in a series of ethanol solutions of increasing concentration (5 min in 50%, 70%, 85%, 95%), immersed 15 min in 100% ethanol, and cleared in methyl salicylate (Thermo Fisher Scientific).

For dopamine and/or glutamate immunofluorescence, the brain was immersed for 2 h at 4°C in a 0.05 M Tris-buffered 0.1% sodium metabisulfite and 0.8% NaCl (TBSM, pH 7.4) solution containing 2% glutaraldehyde. The brain was then transferred to TBSM containing 20% (wt/vol) sucrose overnight at 4°C. The next day, 25-μm-thick brain sections were obtained with a cryostat, collected on glass slides, and air-dried overnight. The sections were then rinsed 3 times 10 min and incubated in a blocking solution composed of TBSM containing 1% sodium borohydride for 30 min. After three rinses in TBSM, the sections were incubated in TBSM containing 5% normal goat serum and 0.3% Triton X-100 for 60 min (blocking solution). The sections were then incubated overnight at 4°C in the blocking solution containing the anti-dopamine and/or anti-glutamate primary antibodies. The next day, the sections were rinsed 3 times 10 min with TBSM, incubated in the blocking solution containing the appropriate secondary antibodies (see below) for 60 min, and rinsed 3 times 10 min in TBSM. The slides were coverslipped using Vectashield as mounting medium (with or without DAPI, H-1200 or H-1000, Vector Laboratories).

For dopamine immunofluorescence, a mouse anti-dopamine primary antibody was used (1:400; MAB5300; Millipore) followed by a either a goat anti-mouse-AlexaFluor-488 (1:400; A11001; Invitrogen) or a goat anti-mouse antibody AlexaFluor-594 (diluted 1:400, 115-585-146, Jackson ImmunoResearch Laboratories). The specificity of the MAB5300 antibody for dopamine was tested using ELISA by the manufacturer (Millipore). The pattern of labeling in our material corresponded to that reported with other DA antibodies in the lamprey (Pierre et al., 1997; Abalo et al., 2005). We previously confirmed that dopamine immunoreactive neurons in the PT express TH (the rate-limiting enzyme for dopamine synthesis) in lampreys (Ryczko et al., 2013, 2017) and salamander (Ryczko et al., 2016c). It is unlikely that the MAB5300 antibody labels noradrenergic fibers in our material because no noradrenergic nucleus equivalent to the locus coeruleus was found in *Petromyzon marinus* using mRNA hybridization (Barreiro-Iglesias et al., 2010). In salamanders, the MAB5300 antibody labels dopaminergic neurons in the PT but not the noradrenergic TH-positive neurons in the locus coeruleus (Ryczko et al., 2016c). For glutamate immunofluorescence, a rabbit anti-glutamate polyclonal primary antibody was used (diluted 1:5000; IG1007, lot 3603, ImmunoSolution) followed by a goat anti-rabbit AlexaFluor-594 antibody (diluted 1:400; A11012, Invitrogen). The IG1007 glutamate antibody was previously used to label glutamatergic neurons in the lamprey brain (Barreiro-Iglesias et al., 2010; Villar-Cerviño et al., 2011; Fernández-López et al., 2012; Ryczko et al., 2017) and in salamanders (Ryczko et al., 2016a). The specificity of the antibody was shown by the supplier who found no immunoreaction against other amino acid conjugates, such as aspartate using dot blots. The labeling obtained was reported to be similar to that obtained with a mouse anti-glutamate monoclonal antibody (Fernández-López et al., 2012). No staining of lamprey brain proteins extracts was revealed by Western blots (Barreiro-Iglesias et al., 2010; Villar-Cerviño et al., 2011). The brain region stained by the antibody in the present study (the PT) contains neurons positive for the vesicular transporter for glutamate mRNA (Villar-Cerviño et al., 2011) and was found to send glutamatergic projections to the MLR using electrophysiological recordings and calcium imaging coupled with pharmacological blockers (Ryczko et al., 2017). Omitting the primary antibody from the procedures resulted in the absence of specific labeling on the brain sections. Biocytin was visualized with streptavidin-AlexaFluor-594, -488, or -350 (diluted 1:400, Invitrogen) added to the solution containing the secondary antibodies without altering the immunofluorescence labeling.

The sections or whole mount were observed and photographed using an E600 epifluorescence microscope equipped with a DXM1200 digital camera (Nikon). For some analyses, a confocal microscope was used (FV1000, Olympus). Photoshop CS5 (Adobe) was used to combine photomicrographs taken with different filter sets and to adjust the intensity levels so that all fluorophores were clearly visible simultaneously.

Statistics. Data in the text are presented as the mean ± SEM. No statistical method was used to predetermine sample sizes, which were similar to those used generally in the field. No randomization or blinding procedure was used. The statistical analysis was done using Sigma Plot 12.5. Correlations between variables and their significance were calculated using the Pearson product moment correlation test. The Shapiro-Wilk test was used to assess normality, and the Levene test was used to assess equal variance. Parametric statistical tests were used when assumptions for normality and equal variance were confirmed. Otherwise, nonparametric analyses were used. To compare the data obtained from dependent groups, we used a parametric one-way ANOVA for repeated measures or a nonparametric Friedman ANOVA on ranks for repeated measures. Both ANOVAs were followed by a Student-Newman-Keuls *post hoc* test for multiple comparisons between groups. Statistical differences were assumed to be significant when $p < 0.05$.

Results

DA innervation of reticular nuclei

The four reticular nuclei (the MRN, ARRN, MRRN, and PRRN) contain the large majority of RS neurons in lampreys (Rovainen, 1967; Nieuwenhuys, 1972, 1977; Brocard and Dubuc, 2003; for review, see Ryczko and Dubuc, 2013). They can be easily delineated for nucleus-specific recording or targeted tracer injections, as shown following injection of a neural tracer (biocytin) at the level of the second spinal segment to retrogradely label RS neurons (Fig. 1*A*,*B*; $n = 5$ animals). To determine whether these four nuclei receive DA innervation, retrograde labeling of RS neurons was coupled with immunofluorescence directed against dopamine, and transverse slices were observed at the level of each reticular nucleus. We found numerous DA fibers and varicosities around the cell bodies and throughout the dendritic trees of RS neurons in the MRN (Fig. 1*C–E*; $n = 4$ animals), ARRN (Fig. 1*F–H*; $n = 4$ animals), MRRN (Fig. 1*I–K*; $n = 4$ animals), and PRRN (Fig. 1*L–N*; $n = 4$ animals). These fibers and varicosities are likely not noradrenergic because, as mentioned above, the locus coeruleus was not found in *Petromyzon marinus* using mRNA ISH (Barreiro-Iglesias et al., 2010) (see also Materials and Methods).

The PT sends descending DA projections to each reticular nucleus

We then looked for the origin of this DA innervation. As mentioned above, a major source of descending DA projections to brainstem networks in lampreys is the PT (Ryczko et al., 2013, 2017; Perez-Fernandez et al., 2014, 2017; von Twickel et al., 2019). To determine whether the PT sends descending

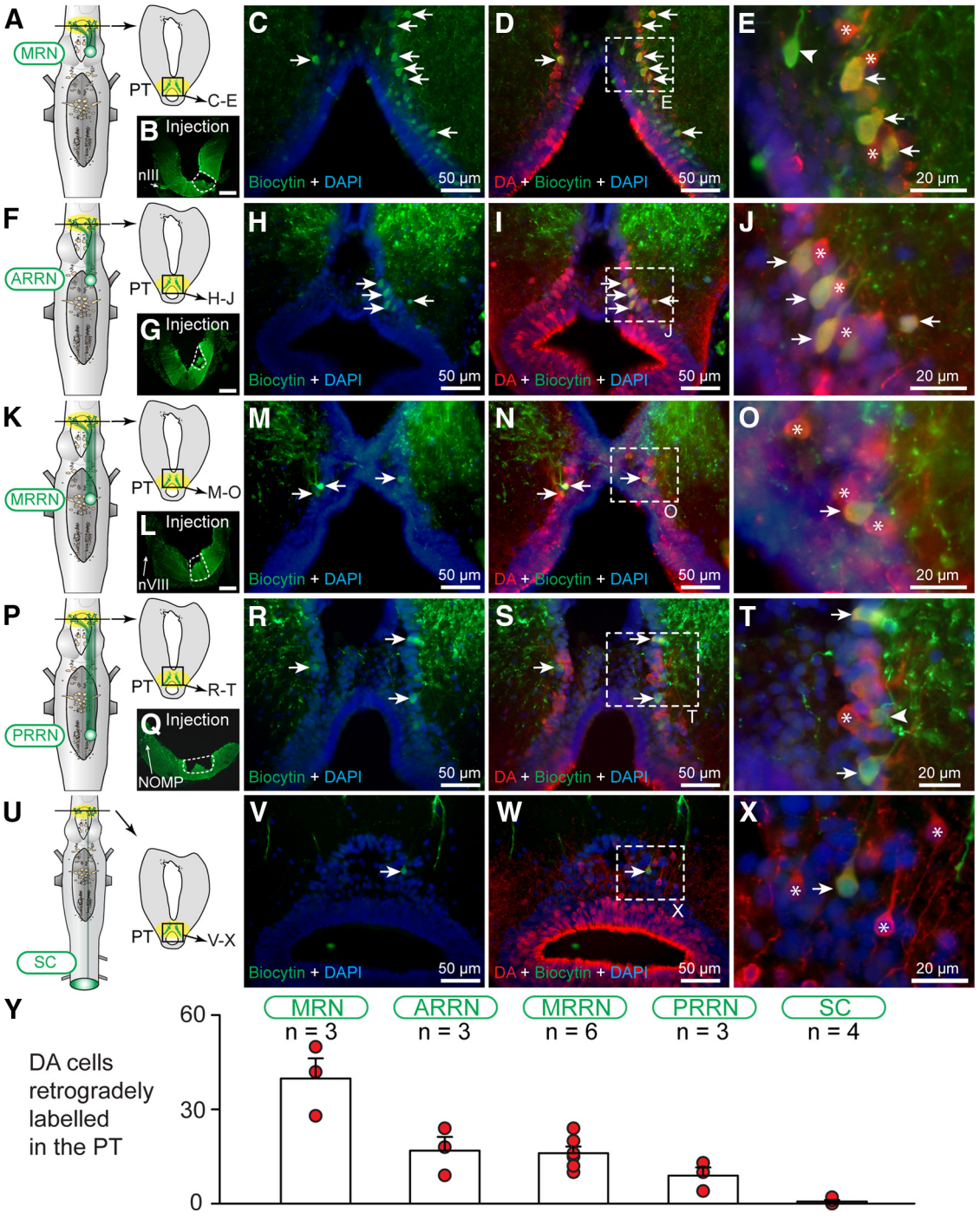

Figure 2. DA-positive neurons in the PT send descending projections to the four reticular nuclei in lampreys. ***A***, ***F***, ***K***, ***P***, Schematic dorsal view of a larval lamprey brain. Right, Diagram represents a cross section at the level of the PT (homologous to the mammalian A9 and/or A10) (see Pombal et al., 1997; Ryczko et al., 2013, 2016c) with the approximate location of the photomicrographs shown in ***C–E***, ***H–J***, ***M–O***, ***R–T***. ***B***, ***G***, ***L***, ***Q***, Photomicrographs represent the tracer (biocytin, green) injection site (enclosed by white dashed lines) in the MRN (***B***), ARRN (***G***), MRRN (***L***), and PRRN (***Q***) of the preparations shown in ***C–E***, ***H–J***, ***M–O***, and ***R–T***, respectively. Scale bar, 200 µm. nIII, Third cranial nerve; nVIII, eighth cranial nerve; NOMP, nucleus octavomotor posterior. For spinal cord (SC) injections, the tracer was applied on the rostral stump after a transverse section at the level of the second spinal segment (***U***). ***C–E***, ***H–J***, ***M–O***, ***R–T***, ***U–X***, Transverse sections represent examples of double labeling of PT cells positive for DA (red) and biocytin (green) that project to the MRN (***C–E***), ARRN (***H–J***), MRRN (***M–O***), PRRN (***R–T***), or spinal cord (***U–X***). ***E***, ***J***, ***O***, ***T***, ***X***, Magnifications of the dashed rectangles in ***D***, ***I***, ***N***, ***S***, and ***W***, respectively. Arrowheads indicate examples of biocytin-labeled neurons. *Examples of DA-positive cells. Arrows indicate examples of double-labeled neurons (DA-positive and biocytin-labeled). Blue represents DAPI. ***Y***, Graph represents the number of DA neurons retrogradely labeled in the PT following an injection of tracer in each reticular nucleus or in the spinal cord (the number of preparations per injection site is indicated). ***B–E***, ***G–J***, ***L–O***, ***Q–T***, and ***V–X***, Data were obtained from five different preparations.

projections to reticular nuclei, we injected a tracer (biocytin) at the level of the dendritic trees of the RS cells in different animal groups. Biocytin-positive neurons were found in the PT following tracer injection in each reticular nucleus (MRN, Fig. 2*A–C*; ARRN, Fig. 2*F–H*; MRRN, Fig. 2*K–M*; PRRN, Fig. 2*P–R*). Neurons positive for biocytin and dopamine (double-labeled cells) were found in the PT following injections in the MRN (40 ± 6 neurons, $n = 3$ animals; Fig. 2*D*,*E*,*Y*), ARRN (17 ± 4

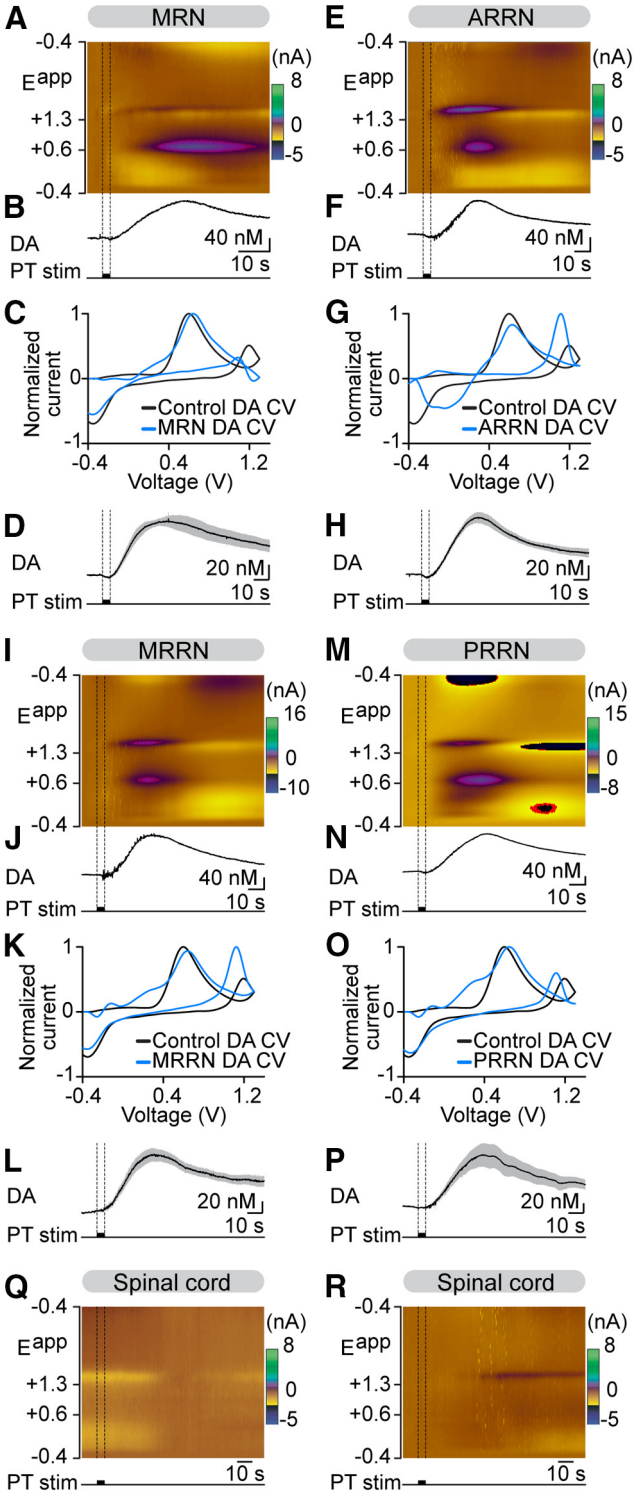

Figure 3. Stimulation of the PT evokes DA release in the four reticular nuclei. ***A***, ***E***, ***I***, ***M***, ***Q***, ***R***, Local activation of cell bodies in the PT by microinjections (0.67–9.78 pmol) of D-glutamate (5 mM) evoked DA release in the MRN (***A***), ARRN (***E***), MRRN (***I***), and PRRN (***M***), but not in the spinal cord (two single trials from two different preparations in ***Q*** and ***R***). The single-trial color plots represent current changes (color) as a function of electrode potential (*y* axis) across time (*x* axis). DA was identified by its oxidation peak (~0.6 V; purple feature). DA was transiently evoked in the reticular nuclei following PT activation. We detected an additional electroactive species (~1.2 V) that we previously identified as hydrogen peroxide (Ryczko et al., 2016c). ***B***, ***F***, ***J***, ***N***, Changes in DA concentration in the reticular nuclei extracted from the data in ***A***, ***E***, ***I***, ***M***. ***C***, ***G***, ***K***, ***O***, Plots of normalized current versus voltage (cyclic voltammogram) obtained from the single trials recorded in each reticular nucleus (in blue) represented in ***A***, ***B***, ***E–F***, ***I–J***, and ***M***, ***N***. The DA signal recorded during these single trials was similar to those induced by a solution of DA (1 μM bath-applied on the electrode in a flow cell, black) in the MRN ($R = 0.92$, $p < 0.001$, ***C***), ARRN ($R = 0.64$, $p < 0.001$, ***G***), MRRN ($R = 0.92$, $p < 0.001$, ***K***), and PRRN ($R = 0.93$, $p < 0.001$, ***O***), thus confirming DA detection in all four reticular nuclei. ***D***, ***H***, ***L***, ***P***, Averaged changes (mean ± SEM) in DA concentration across time in the MRN ($n = 10$ trials from 2 preparations, 5 trials per preparation), ARRN ($n = 15$ trials from 5 preparations, 3 trials per preparation), MRRN ($n = 8$ trials from 4 preparations, 2 trials per preparation), and PRRN ($n = 6$ trials from 3 preparations, 2 trials per preparation) in response to chemical stimulation of the PT with D-glutamate. ***A–D***, ***E–H***, ***I–P***, ***Q***, ***R***, Data were obtained from five different preparations.

neurons, $n = 3$ animals; Fig. 2*I*,*J*,*Y*), MRRN (16 ± 2 neurons, $n = 6$ animals; Fig. 2*N*,*O*,*Y*), and PRRN (9 ± 3 neurons, $n = 3$ animals; Fig. 2*S*,*T*,*Y*). Almost no double-labeled cells were found in the PT when injecting the tracer at the level of the second spinal segment (1 ± 0 neurons, $n = 4$ animals; Fig. 2*U–Y*). Together, this indicates that each reticular nucleus receives descending DA projections from the PT, suggesting that reticular nuclei are possible target sites for dopamine release.

PT stimulation evokes dopamine release in each reticular nucleus

In isolated brain preparations, a fast scan voltammetry electrode was placed in each of the four reticular nuclei, and the PT was stimulated using electrical stimulation. Because electrical stimulation can recruit fibers of passage, in some experiments it was replaced with D-glutamate chemical stimulation to confirm that activation of local cell bodies within the PT was involved in the evoked responses (Ryczko et al., 2013, 2016c, 2017). PT stimulation elicited dopamine release in the MRN (Fig. 3*A–D*; $n = 2$ animals with chemical stimulation, $n = 4$ animals with electrical stimulation), the ARRN (Fig. 3*E–H*; $n = 5$ animals with chemical stimulation), the MRRN (Fig. 3*I–L*; $n = 4$ animals with chemical stimulation, $n = 5$ animals with electrical stimulation), and the PRRN (Fig. 3*M–P*; $n = 3$ animals with chemical stimulation, $n = 5$ animals with electrical stimulation), but not in the spinal cord (Fig. 3*Q*,*R*; $n = 4$ animals with chemical stimulation, $n = 2$ animals with electrical stimulation). We confirmed that the recorded signal was dopamine by comparing it with that evoked by a bath solution of dopamine (1 μM, see Fig. 3*C*,*G*,*K*,*O*) (Ryczko et al., 2013, 2016c). Together, this indicates that each of the four reticular nuclei is a target for the release of dopamine by the descending fibers of PT neurons.

The intensity of PT-evoked swimming is decreased by application of a D_1 antagonist in the MRRN

Previous work showed that PT stimulation evokes MLR and RS activity, as well as locomotion (Derjean et al., 2010; Ryczko et al., 2013, 2016c, 2017). To determine whether dopamine release at the RS level affected PT-evoked swimming activity, a D_1 antagonist (SCH 23390) was bilaterally applied (0.5 mM) over RS neurons. We focused on the MRRN that has been more extensively studied and shown to play a crucial role in the control of locomotion (e.g., Di Prisco et al., 1997; Sirota et al., 2000; Brocard and Dubuc, 2003; Jackson et al., 2007). In semi-intact preparations, where the brain is exposed and the attached body can swim in the recording chamber (Fig. 4*A*,*B*), PT stimulation (2 ms pulses, 5 Hz, 5–13 μA) evoked swimming bouts as previously reported by us (Derjean et al., 2010; Ryczko et al., 2013, 2017). A bilateral microinjection of a D_1 receptor antagonist (SCH 23390, 0.5 mM) over the MRRN reduced by 57% the swimming frequency (1.4 ± 0.1 vs 0.6 ± 0.1 Hz, $p < 0.001$ Student-Newman-

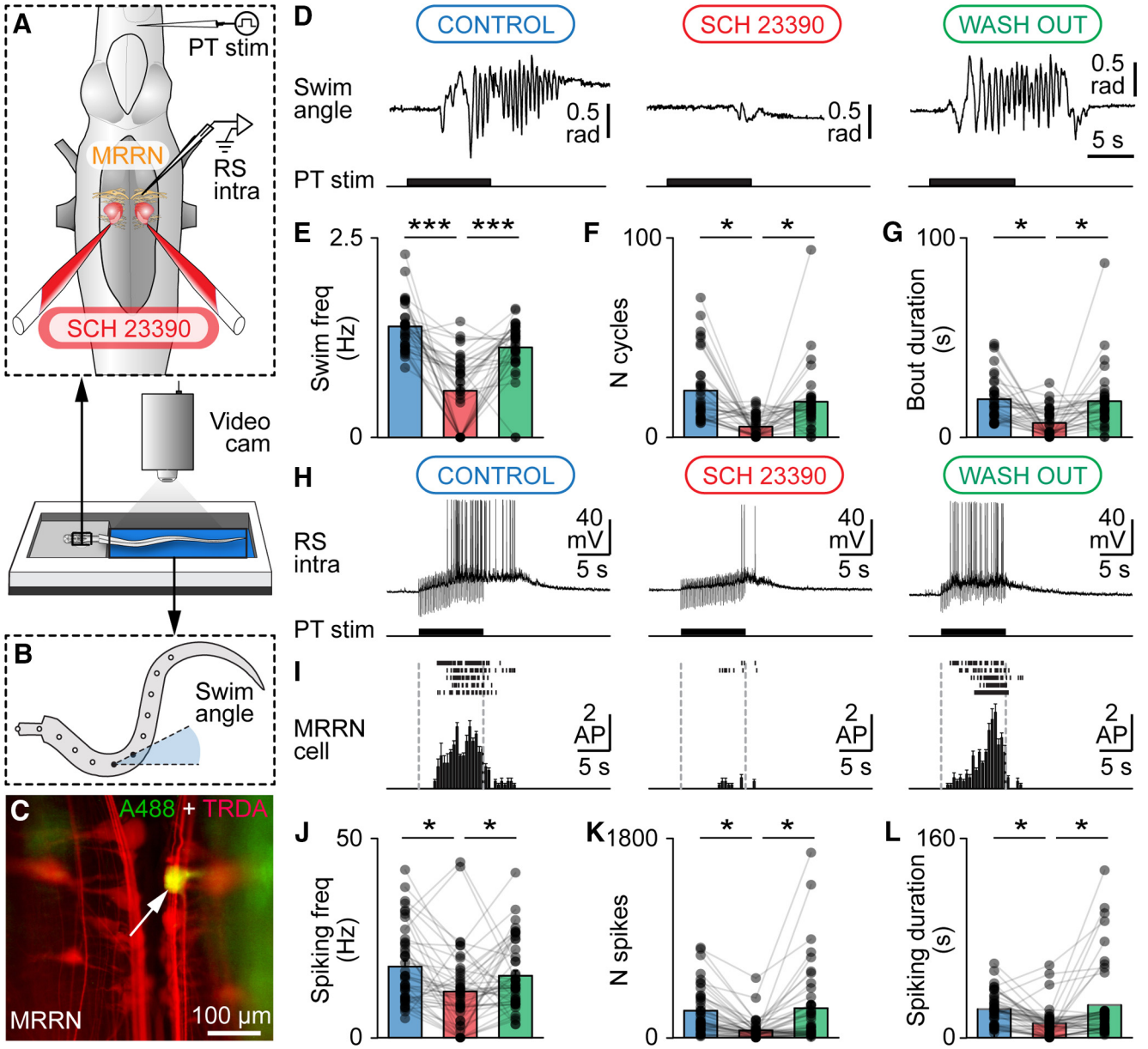

Figure 4. Injection of a D_1 receptor antagonist in the MRRN decreases RS spiking activity and swimming evoked by stimulation of the PT. ***A***, ***B***, In semi-intact lamprey preparations, the PT was stimulated electrically, and swimming was monitored by measuring the angular variations (radians) of body curvature over time. The D_1 antagonist (SCH 23390, 0.5 mM) was bilaterally injected (0.36-0.91 pmol) over the MRRN using a Picospritzer. RS neurons in the MRRN were recorded intracellularly. ***C***, Dorsal view of an MRRN RS neuron (arrow) filled with the intracellular dye biocytin and revealed with Alexa-488 (A488, green) after retrograde labeling with TRDA (red) injection at the level of the second spinal segment, at the end of the experiment. ***D***, Single trials showing the effect of MRRN microinjection of a D_1 antagonist on swimming evoked by PT stimulation (10 s train, 5 Hz, 5 µA, 2 ms pulses). ***E–G***, Bar charts showing the effect of the D_1 antagonist on swimming frequency (***E***), number of locomotor cycles (***F***), and duration of the swimming bout (***G***) in 35 trials (dots) pooled from 7 animals, with 5 trials per condition per animal. ***H***, Single trials showing the effect of MRRN injection of D_1 antagonist on RS spiking activity evoked by PT stimulation (10 s train, 5 Hz, 5 µA, 2 ms pulses). ***I***, Data represent the effect of bilateral injection of a D_1 antagonist over the MRRN on RS spiking activity evoked by PT stimulation, with 5 trials per condition. Top, Scatter plot represents the action potentials (AP). Bottom, Number of AP (±SEM) calculated from the scatter plots shown on top (bin 0.5 s). Gray vertical dotted lines indicate PT stimulation onset and offset. ***J–L***, Bar charts represent the effect of a D_1 antagonist injected bilaterally over the MRRN, on RS spiking frequency (***J***), number of spikes (***K***), and spiking activity duration (***L***) in 45 trials (dots) pooled from 9 animals, with 5 trials per condition per animal. ***D*** and ***H***, ***I***, Data were obtained from two different preparations. *$p < 0.05$; ***$p < 0.001$; Student-Newman Keuls test after a one-way repeated-measures ANOVA or a Friedman one-way repeated-measures ANOVA on ranks ($p < 0.01$ to $p < 0.001$).

Keuls test after a one-way repeated-measures ANOVA, $p < 0.001$, $n = 35$ trials pooled from 7 preparations; Fig. 4*D*,*E*). It reduced by 78% the number of locomotor cycles (23 ± 3 vs 5 ± 1 cycles, $p < 0.05$, Student-Newman-Keuls test after a Friedman one-way repeated-measures ANOVA on ranks, $p < 0.001$; Fig. 4*D*,*F*) and reduced by 62% the duration of the swimming bout (19.1 ± 2.0 vs 7.2 ± 1.2 s, $p < 0.05$, Student-Newman-Keuls test after a Friedman one-way repeated-measures ANOVA on ranks, $p < 0.001$; Fig. 4*D*,*G*). These three locomotor parameters significantly recovered after washout (frequency: 1.1 ± 0.1 Hz, $p < 0.001$ vs injection; number of cycles 18 ± 3, $p < 0.05$ vs injection; bout duration: 18.1 ± 2.6 s, $p < 0.05$ vs injection; Student-Newman-Keuls test for the three parameters; Fig. 4*D*–*G*).

We also determined whether reduced locomotor activity was associated with a decrease in MRRN RS activity using intracellular recordings (Fig. 4*C*). Bilateral injection of the D_1 antagonist

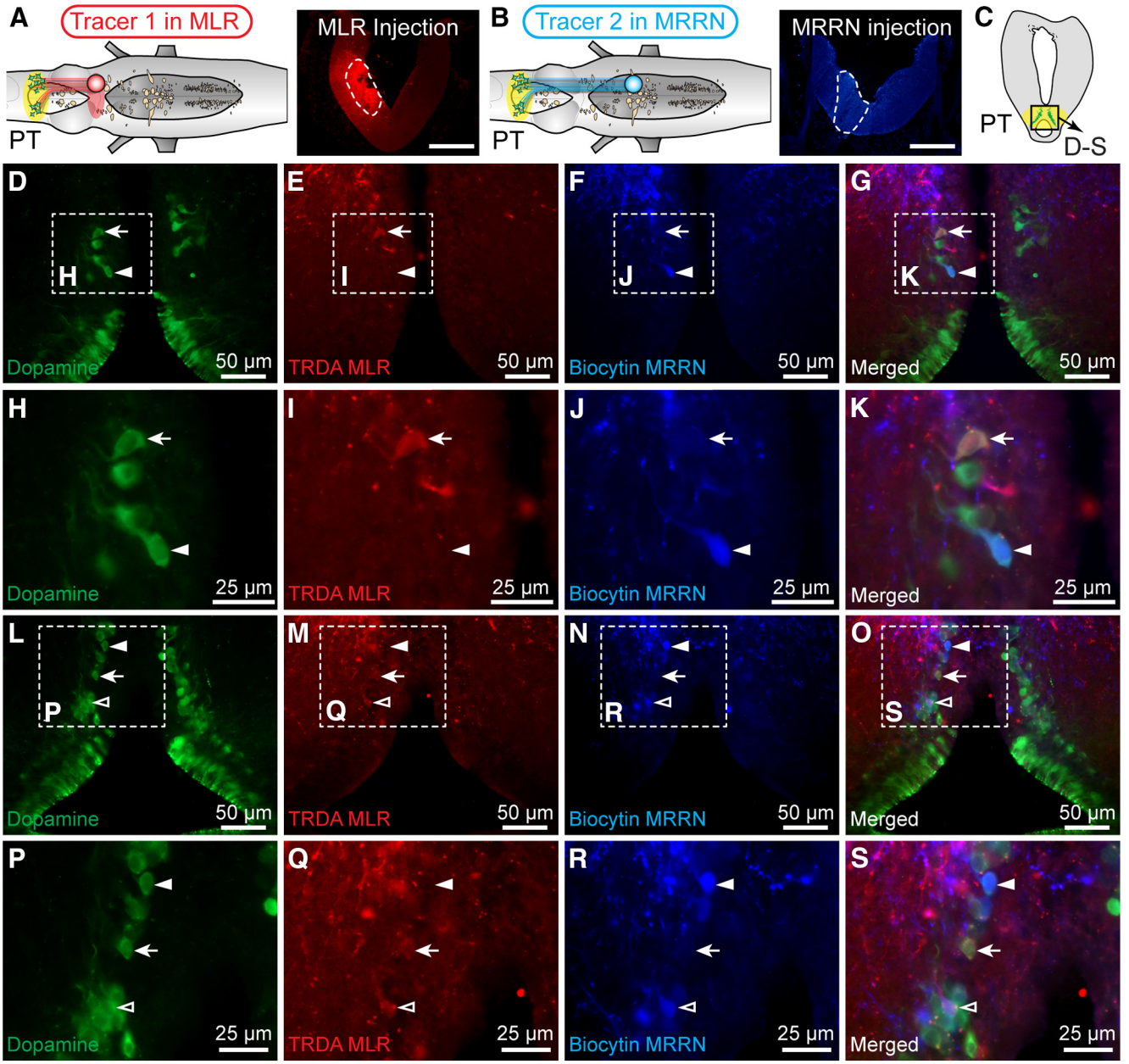

Figure 5. DA projections from the PT to the MLR and MRRN. ***A–C***, In lamprey brainstems, dual retrograde tracing was performed using two different tracers, TRDA, and biocytin, injected in the MLR (i.e., rostral to the giant cell I1) (Ryczko et al., 2013) and in the MRRN, respectively. Photomicrographs represent the injection sites (enclosed by white dashed lines) for TRDA injection in the MLR in ***A***, and for biocytin injection in the MRRN in ***B***. Scale bars, 300 µm. Immunofluorescence against DA was conducted on transverse sections at the level of the PT. ***D–G***, ***L–O***, Triple labeling experiments showing neurons positive for dopamine (green), biocytin (blue), or TRDA (red) and the merged photomicrographs. ***H–K***, ***P–S***, Magnifications of ***D–G*** and ***L–O***, respectively. Arrows indicate neurons retrogradely labeled with TRDA and immunopositive for dopamine. White filled arrowheads indicate cells positive for biocytin and dopamine. White empty arrowheads indicate cells positive for the three markers. ***D–S***, Data were obtained from the same preparation.

over the MRRN reduced by 35% the spiking frequency (17.9 ± 1.4 vs 11.7 ± 1.5 Hz, $p < 0.05$ Student-Newman-Keuls test after a Friedman one-way repeated-measures ANOVA on ranks, $p < 0.001$, $n = 45$ trials pooled from 9 preparations; Fig. 4*H–J*). It also reduced by 73% the number of spikes evoked by PT stimulation (239 ± 31 vs 65 ± 14 spikes, $p < 0.05$ Student-Newman-Keuls test after a Friedman one-way repeated-measures ANOVA on ranks, $p < 0.001$; Fig. 4*H*,*I*,*K*), and reduced by 50% the duration of spiking activity (23.2 ± 1.9 vs 11.6 ± 1.8 s, $p < 0.05$ Student-Newman-Keuls test after a Friedman one-way repeated-measures ANOVA on ranks, $p < 0.001$; Fig. 4*H*,*I*,*L*). These three electrophysiological parameters significantly recovered after washout (spiking frequency 15.6 ± 1.3 Hz, $p < 0.05$ vs injection; number of spikes: 259 ± 53, $p < 0.05$ vs injection; spiking activity duration 26.4 ± 4.6 s, $p < 0.05$ vs injection; Student-Newman-Keuls test for the three parameters; Fig. 4*H–L*). Together, our results suggest that a release of dopamine in the MRRN would contribute to PT-evoked swimming by increasing RS activity through D_1 receptors.

PT sends distinct projections to the MLR and MRRN

We previously reported that PT DA cells project extensively to the MLR (Ryczko et al., 2013, 2017). To determine whether the same PT neurons project to the MLR and to reticular nuclei, we used dual retrograde tracing with two different tracers. A first tracer was injected in the MRRN and a second one in the MLR.

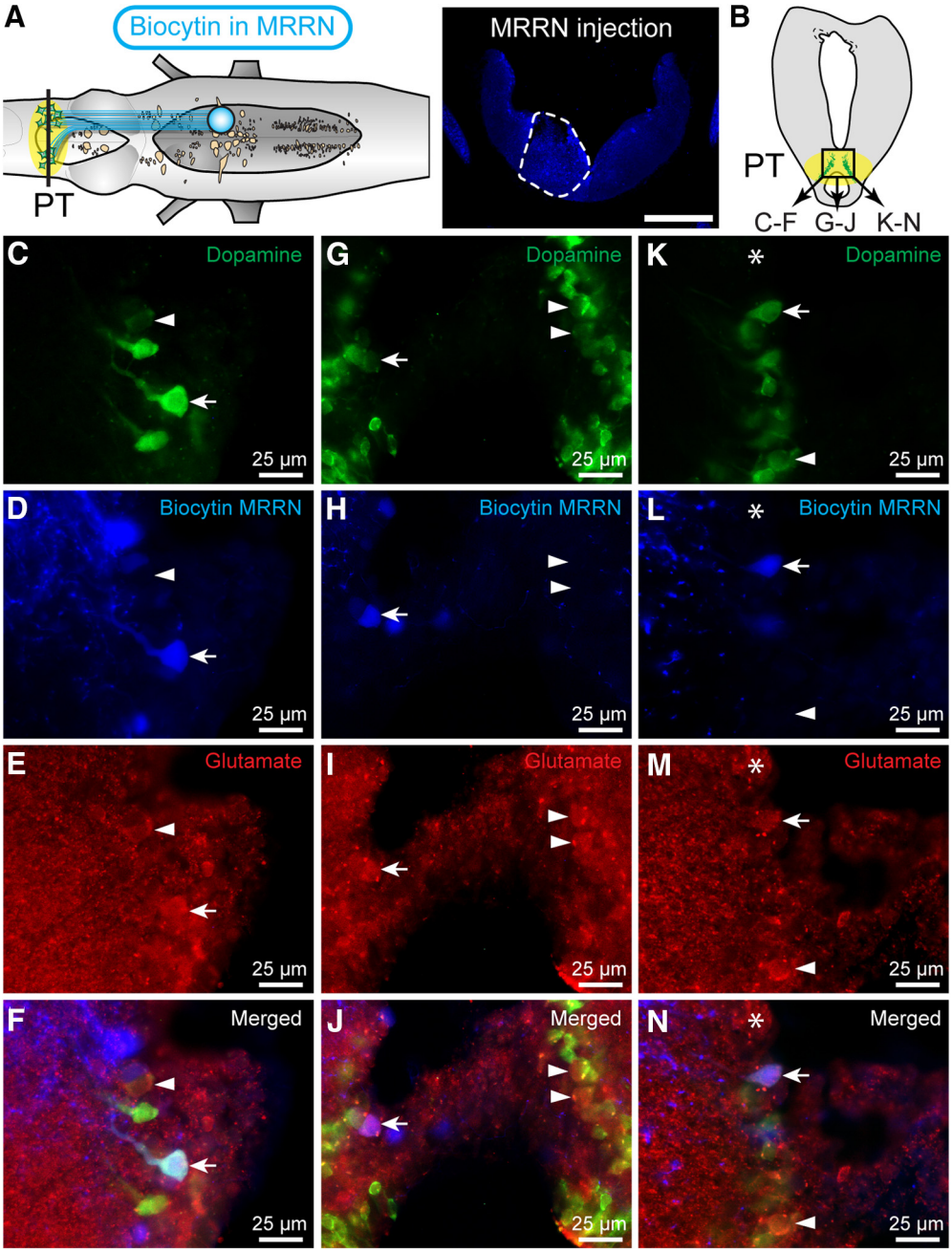

Figure 6. Coexpression of glutamate by DA neurons of the PT projecting to the MRRN. ***A***, In lamprey brainstems, a tracer (biocytin) was injected in the MRRN. Photomicrograph represents the injection site enclosed by a white dashed line. Scale bar, 300 µm. ***B***, Immunofluorescence against glutamate and dopamine was conducted on brain sections at the level of the PT. ***C–N***, Photomicrographs showing cells positive for dopamine (***C–F***, green), biocytin (***G–J***, blue), and glutamate (***K–N***, red), as well as the merged photomicrographs. Arrowheads indicate cells positive for dopamine and glutamate. *Cell only positive for glutamate. Arrows indicate cells positive for the three markers. ***A–N***, Data were obtained from two different preparations.

Among the PT DA neurons, only 14 ± 4% projecting to the MRRN also projected to the MLR (1/12, 2/16, 5/24 DA neurons, $n = 3$ animals) (Fig. 5*A–S*), suggesting that descending DA inputs to the MLR and reticular nuclei originate mostly from distinct DA cells.

We previously reported that single PT DA neurons send a dual DA/glutamatergic drive to the MLR (Ryczko et al., 2017). We next examined whether such dual projections could also target a reticular nucleus. Using tracer injection in the MRRN coupled with DA/glutamate immunofluorescence in the PT, we found triple-labeled neurons in the PT (Fig. 6*A–N*), suggesting that dual DA/glutamatergic projections from the PT to the reticular nuclei are likely present.

Discussion

In the present study, we show in lampreys that meso-diencephalic DA neurons send descending DA fibers to the four reticular nuclei (MRN, ARRN, MRRN, PRRN), in which RS neurons are located. We show that these descending projections release dopamine in each of the reticular nuclei. Blockade of D_1 receptors was tested in the MRRN, a reticular nucleus known to play a key role in locomotor control, and we found that it reduced RS spiking and decreased the swimming frequency, the number of locomotor cycles, and the duration of PT-evoked swimming. This indicates that descending DA inputs to RS neurons play a role in locomotor control in lampreys.

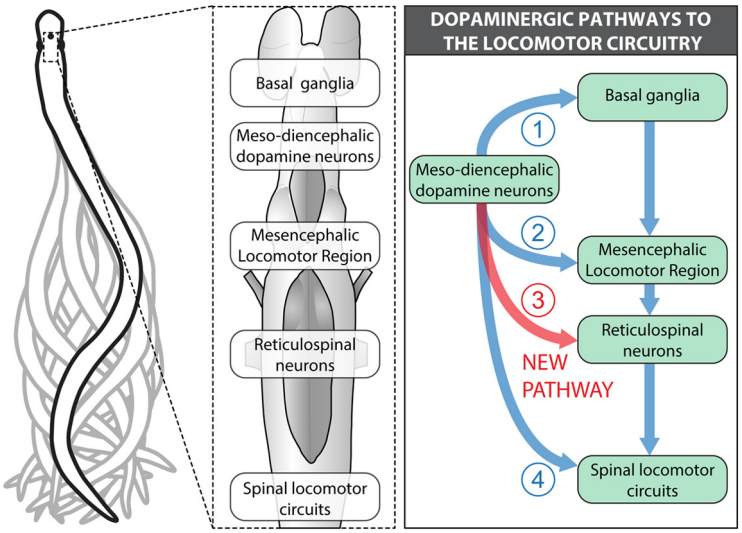

Figure 7. The DA pathways projecting to the locomotor circuitry. Arrow 1 indicates the well-known ascending DA pathways from A8/A9/A10 to the basal ganglia (lamprey: DA source, PT, see Pombal et al., 1997; Ryczko et al., 2013; mammalian DA source: A8/A9/A10, see Poirier and Sourkes, 1965; Sourkes and Poirier, 1965; for review, see Fahn, 2015) that in turn project down to the MLR (lamprey: see Stephenson-Jones et al., 2011; mouse: see Roseberry et al., 2016). Arrow 2 indicates the descending DA pathway to the MLR recently uncovered in our previous studies and that of others (lamprey DA source: PT, see Ryczko et al., 2013, 2017; Perez-Fernandez et al., 2014; salamander DA source: PT, see Ryczko et al., 2016c; rodent DA sources: A8/A9, see Ryczko et al., 2016c in rats; A13, see Sharma et al., 2018 in mice). Arrow 3 indicates the descending DA pathway to RS neurons uncovered in the present study. Arrow 4 indicates the descending DA pathway to spinal locomotor circuits. In mammals, A11 send descending projections to the spinal cord, and optogenetic activation of A11 DA neurons increases locomotor activity *in vivo* (mouse: see Koblinger et al., 2014, 2018). In zebrafish, dopamine increases the excitability of motoneurons via D_1 receptors (Jha and Thirumalai, 2020). In lampreys, descending DA projections to the spinal cord likely do not originate from the PT (only 1 ± 0 cells found here), but from a distinct diencephalic group of periventricular DA cells of the mammillary area (Barreiro-Iglesias et al., 2010).

Comparative aspects

The descending DA pathway from the PT to reticular nuclei could be present in all vertebrates. The lamprey is one of the phylogenetically oldest vertebrates, and its nervous system is considered the blueprint of the mammalian brain (Robertson et al., 2014). We previously showed that the descending DA pathway from meso-diencephalic DA neurons to the MLR found in lampreys (Ryczko et al., 2013, 2017; Perez-Fernandez et al., 2014) is conserved in amphibians, mammals, and likely humans (Ryczko et al., 2016c; see also Sharma et al., 2018; for review, see Ryczko and Dubuc, 2017). Whether the meso-diencephalic DA inputs to the MLR promote locomotor output in mammals as in lampreys remain to be determined. In addition to the innervation of the MLR, it appears that another DA descending projection, originating from a different DA nucleus (A11) and innervating the spinal cord, is conserved in vertebrates. For instance, the spinal cord of lampreys receives descending projections from a distinct set of periventricular DA neurons in the mammillary area (Barreiro-Iglesias et al., 2010) that do not project to the MLR or striatum (Ryczko et al., 2013, 2016c). Whether these DA neurons correspond to A11 in mammals (see e.g., Koblinger et al., 2014, 2018) needs to be examined in further details. This hypothesis concurs with our present observation that stimulation of the PT does not evoke dopamine release in the spinal cord.

The homology between reticular nuclei in lampreys and mammals is not fully resolved. Based on the anatomic organization of reticular nuclei, the ARRN and MRRN would constitute the pontine reticular formation (respectively homologous to the nucleus reticular pontis oralis and nucleus reticular pontis caudalis). The PRRN is considered part of the medullary reticular formation (Brocard and Dubuc, 2003; for review, see Cruce and Newman, 1984; Brownstone and Chopek, 2018). The DA innervation of reticular nuclei has not received much attention in mammals. A recent tracing study in mice indicates that only a few neurons from A13 send DA fibers to the medullary reticular formation, suggesting that another DA nucleus is the source of the DA innervation of this reticular nucleus (Sharma et al., 2018).

Functional significance

RS neurons constitute the final common descending pathway carrying locomotor commands to the spinal cord (for review, see Dubuc et al., 2008). They integrate sensory inputs and descending commands, and shape motor output by sending monosynaptic input to spinal interneurons and motoneurons (Buchanan and Grillner, 1987; for review, see Brownstone and Chopek, 2018). RS neurons receive inputs from the MLR (e.g., Shik et al., 1966; Sirota et al., 2000; Cabelguen et al., 2003; Bretzner and Brownstone, 2013, Ryczko et al., 2016a; for review, see Ryczko and Dubuc, 2013), the diencephalic locomotor region (El Manira et al., 1997; Ménard and Grillner, 2008), also called subthalamic locomotor region (Parker and Sinnamon, 1983; Milner and Mogenson, 1988), and the less studied cerebellar locomotor region (Mori et al., 1998, 1999). RS neurons also control steering movements, by modulating body bending, with RS activity increasing ipsilaterally to the turn in lampreys (Deliagina et al., 2000; Fagerstedt et al., 2001), fish (Thiele et al., 2014), and salamander (Ryczko et al., 2016b). Future studies should examine whether the DA pathway reported here influences the processing of all the aforementioned functions.

RS neurons also integrate many sensory inputs that shape motor output (e.g., Di Prisco et al., 1994, 2000; Antri et al., 2008; Le Ray et al., 2010; for review, see Daghfous et al., 2016). Previous studies in teleosts showed that dopamine increases synaptic responses evoked by vestibulocochlear stimulation in the Mauthner cell (a large RS neuron in fish) through D_1 receptors (Pereda et al., 1992, 1994; Kumar and Faber, 1999). Fibers positive for TH were observed around Mauthner cell bodies and dendrites in teleosts (McLean and Fetcho, 2004). The present study provides a possible source for descending DA projections to RS neurons. Beyond RS neurons, such modulation of sensory processing in the brainstem by descending DA projections is consistent with a recent study in lampreys showing that visuomotor transformation is modulated by descending DA inputs from the PT to the optic tectum (superior colliculus in mammals) (Perez-Fernandez et al., 2017; see also von Twickel et al., 2019). The pathway reported here allows DA cells to modulate RS activity in response to sensory inputs. This adds up to the previously reported DA innervation of the MLR, through which locomotion

initiation is modulated according to the internal goals of the animal.

The emerging diversity of DA pathways innervating different levels of the locomotor circuitry raises new questions about the conditions in which each DA pathway is recruited to modulate behavior. The different sets of inputs that DA nuclei (A8, A9, A13, A11) receive should offer a substrate for context-specific control of behavior (for review, see Kim et al., 2017; Fougère et al., 2019). Even within a single nucleus, different DA cells can innervate different neural circuits. For instance, in lampreys, the PT sends DA projections to the striatum (Pombal et al., 1997; Ryczko et al., 2013; Perez-Fernandez et al., 2014), the MLR (Ryczko et al., 2013, 2017; Perez-Fernandez et al., 2014), the reticular nuclei (present study), and the optic tectum (Perez-Fernandez et al., 2017; von Twickel et al., 2019). Some DA neurons project both to the MLR and striatum in lampreys (Ryczko et al., 2013) (in rats as well, see Ryczko et al., 2016c), whereas some DA neurons project both to the striatum and optic tectum in lampreys (Perez-Fernandez et al., 2017; von Twickel et al., 2019). In this study, we report that only a small proportion of DA neurons (<15%) projecting to the MRRN also projected to the MLR, suggesting that these DA pathways are mostly segregated. The role of DA neurons projecting to both structures (MLR and reticular formation) versus those projecting to a single structure remains an open question. Moreover, even a single DA neuron often expresses more than a single neurotransmitter. DA neurons coexpressing glutamate or GABA were found in many species (for review, see Morales and Root, 2014; Vaaga et al., 2014). In lampreys, many PT DA neurons projecting to the MLR are also glutamatergic, and we know that glutamate plays a key role in the graded activation of MLR cells and swimming movements (Ryczko et al., 2017). The present anatomic results suggest that some DA neurons send a dual glutamatergic/DA drive to the reticular nuclei as well. However, glutamate is also well known to be present in GABA neurons, although it is not coreleased. Future physiological studies should be aimed at determining whether dopamine and glutamate are coreleased (Ryczko et al., 2017). Whether DA neurons expressing a single versus multiple transmitters play different roles in the control of behavior also remains to be determined. Finally, within a single lamprey DA neuron, dual glutamatergic/DA branches are found in the striatum, whereas "purely" DA branches are found only in the optic tectum (Perez-Fernandez et al., 2017; von Twickel et al., 2019). Whether and how DA neurons exert circuit-specific neurotransmitter release remain to be determined, and future studies are needed.

In conclusion, our study provides evidence that RS neurons receive direct inputs from meso-diencephalic DA neurons, which therefore have access to several levels of the locomotor circuitry (Fig. 7), including the basal ganglia (e.g., Kravitz et al., 2010), MLR (Ryczko et al., 2013, 2016c, 2017; Perez-Fernandez et al., 2014; Sharma et al., 2018), reticular nuclei (present study), and spinal cord circuits (Koblinger et al., 2018; Jha and Thirumalai, 2020). We previously showed that DA inputs provide additional excitation to MLR cells, and in the present study we show a similar effect on RS neurons. It appears therefore that DA inputs to brainstem locomotor circuits make them "ready-to-go," when the decision to move is initiated by the basal ganglia circuits (Fougère et al., 2019). Such function could explain why drugs increasing the concentration of dopamine at the synapse increase locomotor behavior, and why DA cell loss translates into severe locomotor deficits, such as those reported in Parkinson's disease.

References

Abalo XM, Villar-Cheda B, Anadón R, Rodicio MC (2005) Development of the dopamine-immunoreactive system in the central nervous system of the sea lamprey. Brain Res Bull 66:560–564.

Antri M, Auclair F, Albrecht J, Djeudjang N, Dubuc R (2008) Serotoninergic modulation of sensory transmission to brainstem reticulospinal cells. Eur J Neurosci 28:655–667.

Barreiro-Iglesias A, Laramore C, Shifman MI, Anadón R, Selzer ME, Rodicio MC (2010) The sea lamprey tyrosine hydroxylase: cDNA cloning and in situ hybridization study in the brain. Neuroscience 168:659–669.

Bretzner F, Brownstone RM (2013) Lhx3-Chx10 reticulospinal neurons in locomotor circuits. J Neurosci 33:14681–14692.

Brocard F, Dubuc R (2003) Differential contribution of reticulospinal cells to the control of locomotion induced by the mesencephalic locomotor region. J Neurophysiol 90:1714–1727.

Brocard F, Ryczko D, Fenelon K, Hatem R, Gonzales D, Auclair F, Dubuc R (2010) The transformation of a unilateral locomotor command into a symmetrical bilateral activation in the brainstem. J Neurosci 30:523–533.

Brownstone RM, Chopek JW (2018) Reticulospinal systems for tuning motor commands. Front Neural Circuits 12:30.

Buchanan JT, Grillner S (1987) Newly identified 'glutamate interneurons' and their role in locomotion in the lamprey spinal cord. Science 236:312–314.

Cabelguen JM, Bourcier-Lucas C, Dubuc R (2003) Bimodal locomotion elicited by electrical stimulation of the midbrain in the salamander *Notophthalmus viridescens*. J Neurosci 23:2434–2439.

Caggiano V, Leiras R, Goni-Erro H, Masini D, Bellardita C, Bouvier J, Caldeira V, Fisone G, Kiehn O (2018) Midbrain circuits that set locomotor speed and gait selection. Nature 553:455–460.

Carlsson A, Lindqvist M, Magnusson T, Waldeck B (1958) On the presence of 3-hydroxytyramine in brain. Science 127:471.

Cruce WL, Newman DB (1984) Evolution of motor systems: the reticulospinal pathways. Am Zool 24:733–753.

Daghfous G, Green WW, Alford ST, Zielinski BS, Dubuc R (2016) Sensory activation of command cells for locomotion and modulatory mechanisms: lessons from lampreys. Front Neural Circuits 10:18.

Deliagina TG, Zelenin PV, Fagerstedt P, Grillner S, Orlovsky GN (2000) Activity of reticulospinal neurons during locomotion in the freely behaving lamprey. J Neurophysiol 83:853–863.

Derjean D, Moussaddy A, Atallah E, St-Pierre M, Auclair F, Chang S, Ren X, Zielinski B, Dubuc R (2010) A novel neural substrate for the transformation of olfactory inputs into motor output. PLoS Biol 8:e1000567.

Di Prisco GV, Dubuc R, Grillner S (1994) 5-HT innervation of reticulospinal neurons and other brainstem structures in lamprey. J Comp Neurol 342:23–34.

Di Prisco GV, Pearlstein E, Robitaille R, Dubuc R (1997) Role of sensory-evoked NMDA plateau potentials in the initiation of locomotion. Science 278:1122–1125.

Di Prisco GV, Pearlstein E, Le Ray D, Robitaille R, Dubuc R (2000) A cellular mechanism for the transformation of a sensory input into a motor command. J Neurosci 20:8169–8176.

Dubuc R (2009) Locomotor regions in the midbrain (MLR) and diencephalon (DLR). In: Encyclopedia of neuroscience (Binder MD, Hirokawa N, Windhorst U, eds), pp 2167–2171. Berlin: Springer.

Dubuc R, Brocard F, Antri M, Fenelon K, Gariépy JF, Smetana R, Ménard A, Le Ray D, Viana Di Prisco G, Pearlstein E, Sirota MG, Derjean D, St-Pierre M, Zielinski B, Auclair F, Veilleux D (2008) Initiation of locomotion in lampreys. Brain Res Rev 57:172–182.

El Manira A, Pombal MA, Grillner S (1997) Diencephalic projection to reticulospinal neurons involved in the initiation of locomotion in adult lampreys *Lampetra fluviatilis*. J Comp Neurol 389:603–616.

Fagerstedt P, Orlovsky GN, Deliagina TG, Grillner S, Ullen F (2001) Lateral turns in the lamprey: II. Activity of reticulospinal neurons during the generation of fictive turns. J Neurophysiol 86:2257–2265.

Fahn S (2015) The medical treatment of Parkinson disease from James Parkinson to George Cotzias. Mov Disord 30:4–18.

Fernández-López B, Villar-Cerviño V, Valle-Maroto SM, Barreiro-Iglesias A, Anadón R, Rodicio MC (2012) The Glutamatergic Neurons in the

Spinal Cord of the Sea Lamprey: An In Situ Hybridization and Immunohistochemical Study. PLOS ONE 7:e47898.
Fougère M, Flaive A, Frigon A, Ryczko D (2019) Descending dopaminergic control of brainstem locomotor circuits. Curr Opin Physiol 8:30–35.
Garcia-Rill E, Houser CR, Skinner RD, Smith W, Woodward DJ (1987) Locomotion-inducing sites in the vicinity of the pedunculopontine nucleus. Brain Res Bull 18:731–738.
Gariépy JF, Missaghi K, Chevallier S, Chartre S, Robert M, Auclair F, Lund JP, Dubuc R (2012a) Specific neural substrate linking respiration to locomotion. Proc Natl Acad Sci USA 109:E84–E92.
Gariépy JF, Missaghi K, Chartre S, Robert M, Auclair F, Dubuc R (2012b) Bilateral connectivity in the brainstem respiratory networks of lampreys. J Comp Neurol 520:1442–1456.
Grätsch S, Auclair F, Demers O, Auguste E, Hanna A, Buschges A, Dubuc R (2019) A brainstem neural substrate for stopping locomotion. J Neurosci 39:1044–1057.
Hagglund M, Borgius L, Dougherty KJ, Kiehn O (2010) Activation of groups of excitatory neurons in the mammalian spinal cord or hindbrain evokes locomotion. Nat Neurosci 13:246–252.
Jackson AW, Pino FA, Wiebe ED, McClellan AD (2007) Movements and muscle activity initiated by brain locomotor areas in semi-intact preparations from larval lamprey. J Neurophysiol 97:3229–3241.
Jha U, Thirumalai V (2020) Neuromodulatory selection of motor neuron recruitment patterns in a visuomotor behavior increases speed. Curr Biol 30:788–801.e3.
Josset N, Roussel M, Lemieux M, Lafrance-Zoubga D, Rastqar A, Bretzner F (2018) Distinct contributions of mesencephalic locomotor region nuclei to locomotor control in the freely behaving mouse. Curr Biol 28:884–901.e883.
Juvin L, Grätsch S, Trillaud-Doppia E, Gariépy JF, Büschges A, Dubuc R (2016) A specific population of reticulospinal neurons controls the termination of locomotion. Cell Rep 15:2377–2386.
Kim LH, Sharma S, Sharples SA, Mayr KA, Kwok CH, Whelan PJ (2017) Integration of descending command systems for the generation of context-specific locomotor behaviors. Front Neurosci 11:581.
Kimura Y, Satou C, Fujioka S, Shoji W, Umeda K, Ishizuka T, Yawo H, Higashijima S (2013) Hindbrain V2a neurons in the excitation of spinal locomotor circuits during zebrafish swimming. Curr Biol 23:843–849.
Kinkhabwala A, Riley M, Koyama M, Monen J, Satou C, Kimura Y, Higashijima S, Fetcho J (2011) A structural and functional ground plan for neurons in the hindbrain of zebrafish. Proc Natl Acad Sci USA 108:1164–1169.
Koblinger K, Fuzesi T, Ejdrygiewicz J, Krajacic A, Bains JS, Whelan PJ (2014) Characterization of A11 neurons projecting to the spinal cord of mice. PLoS One 9:e109636.
Koblinger K, Jean-Xavier C, Sharma S, Fuzesi T, Young L, Eaton SE, Kwok CH, Bains JS, Whelan PJ (2018) Optogenetic activation of A11 region increases motor activity. Front Neural Circuits 12:86.
Kravitz AV, Freeze BS, Parker PR, Kay K, Thwin MT, Deisseroth K, Kreitzer AC (2010) Regulation of parkinsonian motor behaviours by optogenetic control of basal ganglia circuitry. Nature 466:622–626.
Kumar SS, Faber DS (1999) Plasticity of first-order sensory synapses: interactions between homosynaptic long-term potentiation and heterosynaptically evoked dopaminergic potentiation. J Neurosci 19:1620–1635.
Le Ray D, Juvin L, Boutin T, Auclair F, Dubuc R (2010) A neuronal substrate for a state-dependent modulation of sensory inputs in the brainstem. Eur J Neurosci 32:53–59.
Le Ray D, Brocard F, Bourcier-Lucas C, Auclair F, Lafaille P, Dubuc R (2003) Nicotinic activation of reticulospinal cells involved in the control of swimming in lampreys. Eur J Neurosci 17:137–148.
McLean DL, Fetcho JR (2004) Relationship of tyrosine hydroxylase and serotonin immunoreactivity to sensorimotor circuitry in larval zebrafish. J Comp Neurol 480:57–71.
Ménard A, Grillner S (2008) Diencephalic locomotor region in the lamprey: afferents and efferent control. J Neurophysiol 100:1343–1353.
Milner KL, Mogenson GJ (1988) Electrical and chemical activation of the mesencephalic and subthalamic locomotor regions in freely moving rats. Brain Res 452:273–285.
Morales M, Root DH (2014) Glutamate neurons within the midbrain dopamine regions. Neuroscience 282:60–68.
Mori S, Matsui T, Kuze B, Asanome M, Nakajima K, Matsuyama K (1998) Cerebellar-induced locomotion: reticulospinal control of spinal rhythm generating mechanism in cats. Ann NY Acad Sci 860:94–105.
Mori S, Matsui T, Kuze B, Asanome M, Nakajima K, Matsuyama K (1999) Stimulation of a restricted region in the midline cerebellar white matter evokes coordinated quadrupedal locomotion in the decerebrate cat. J Neurophysiol 82:290–300.
Nieuwenhuys R (1972) Topological analysis of the brain stem of the lamprey *Lampetra fluviatilis*. J Comp Neurol 145:165–177.
Nieuwenhuys R (1977) The brain of the lamprey in a comparative perspective. Ann NY Acad Sci 299:97–145.
Ohta Y, Grillner S (1989) Monosynaptic excitatory amino acid transmission from the posterior rhombencephalic reticular nucleus to spinal neurons involved in the control of locomotion in lamprey. J Neurophysiol 62:1079–1089.
Orlovskiĭ GN (1970) Work of reticulo-spinal neurons during locomotion. Biofizika 15:728–737.
Parker SM, Sinnamon HM (1983) Forward locomotion elicited by electrical stimulation in the diencephalon and mesencephalon of the awake rat. Physiol Behav 31:581–587.
Pereda A, Triller A, Korn H, Faber DS (1992) Dopamine enhances both electrotonic coupling and chemical excitatory postsynaptic potentials at mixed synapses. Proc Natl Acad Sci USA 89:12088–12092.
Pereda AE, Nairn AC, Wolszon LR, Faber DS (1994) Postsynaptic modulation of synaptic efficacy at mixed synapses on the Mauthner cell. J Neurosci 14:3704–3712.
Perez-Fernandez J, Stephenson-Jones M, Suryanarayana SM, Robertson B, Grillner S (2014) Evolutionarily conserved organization of the dopaminergic system in lamprey: SNc/VTA afferent and efferent connectivity and D2 receptor expression. J Comp Neurol 522:3775–3794.
Perez-Fernandez J, Kardamakis AA, Suzuki DG, Robertson B, Grillner S (2017) Direct dopaminergic projections from the SNc modulate visuomotor transformation in the lamprey tectum. Neuron 96:910–924.e915.
Pierre J, Mahouche M, Suderevskaya EI, Repérant J, Ward R (1997) Immunocytochemical localization of dopamine and its synthetic enzymes in the central nervous system of the lamprey *Lampetra fluviatilis*. J Comp Neurol 380:119–135.
Poirier L, Sourkes TL (1965) Influence of the substantia nigra on the catecholamine content of the striatum. Brain 88:181–192.
Pombal MA, El Manira A, Grillner S (1997) Afferents of the lamprey striatum with special reference to the dopaminergic system: a combined tracing and immunohistochemical study. J Comp Neurol 386:71–91.
Robertson B, Kardamakis A, Capantini L, Perez-Fernandez J, Suryanarayana SM, Wallen P, Stephenson-Jones M, Grillner S (2014) The lamprey blueprint of the mammalian nervous system. Prog Brain Res 212:337–349.
Roitman MF, Wheeler RA, Wightman RM, Carelli RM (2008) Real-time chemical responses in the nucleus accumbens differentiate rewarding and aversive stimuli. Nat Neurosci 11:1376–1377.
Rolland AS, Tandé D, Herrero MT, Luquin MR, Vazquez-Claverie M, Karachi C, Hirsch EC, François C (2009) Evidence for a dopaminergic innervation of the pedunculopontine nucleus in monkeys, and its drastic reduction after MPTP intoxication. J Neurochem 110:1321–1329.
Roseberry TK, Lee AM, Lalive AL, Wilbrecht L, Bonci A, Kreitzer AC (2016) Cell-type-specific control of brainstem locomotor circuits by basal ganglia. Cell 164:526–537.
Rovainen CM (1967) Physiological and anatomical studies on large neurons of central nervous system of the sea lamprey (*Petromyzon marinus*): I. Müller and Mauthner cells. J Neurophysiol 30:1000–1023.
Ryczko D, Dubuc R (2013) The multifunctional mesencephalic locomotor region. Curr Pharm Des 19:4448–4470.
Ryczko D, Dubuc R (2017) Dopamine and the brainstem locomotor networks: from lamprey to human. Front Neurosci 11:295.
Ryczko D, Grätsch S, Auclair F, Dube C, Bergeron S, Alpert MH, Cone JJ, Roitman MF, Alford S, Dubuc R (2013) Forebrain dopamine neurons project down to a brainstem region controlling locomotion. Proc Natl Acad Sci USA 110:E3235–E3242.
Ryczko D, Auclair F, Cabelguen JM, Dubuc R (2016a) The mesencephalic locomotor region sends a bilateral glutamatergic drive to hindbrain reticulospinal neurons in a tetrapod. J Comp Neurol 524:1361–1383.
Ryczko D, Thandiackal R., Ijspeert AJ (2016b) Interfacing a salamander brain with a salamander-like robot: control of speed and direction with calcium signals from brainstem reticulospinal neurons. In: 2016 6th IEEE International Conference on Biomedical Robotics and Biomechatronics (BioRob), pp 1140–1147.

Ryczko D, Cone JJ, Alpert MH, Goetz L, Auclair F, Dube C, Parent M, Roitman MF, Alford S, Dubuc R (2016c) A descending dopamine pathway conserved from basal vertebrates to mammals. Proc Natl Acad Sci USA 113:E2440–E2449.

Ryczko D, Grätsch S, Schlager L, Keuyalian A, Boukhatem Z, Garcia C, Auclair F, Buschges A, Dubuc R (2017) Nigral glutamatergic neurons control the speed of locomotion. J Neurosci 37:9759–9770.

Sharma S, Kim LH, Mayr KA, Elliott DA, Whelan PJ (2018) Parallel descending dopaminergic connectivity of A13 cells to the brainstem locomotor centers. Sci Rep 8:7972.

Shik ML, Severin FV, Orlovskiĭ GN (1966) Control of walking and running by means of electric stimulation of the midbrain. Biofizika 11:659–666.

Sholomenko GN, Funk GD, Steeves JD (1991) Avian locomotion activated by brainstem infusion of neurotransmitter agonists and antagonists: II. Gamma-aminobutyric acid. Exp Brain Res 85:674–681.

Sinkala E, McCutcheon JE, Schuck MJ, Schmidt E, Roitman MF, Eddington DT (2012) Electrode calibration with a microfluidic flow cell for fast-scan cyclic voltammetry. Lab Chip 12:2403–2408.

Sirota MG, Di Prisco GV, Dubuc R (2000) Stimulation of the mesencephalic locomotor region elicits controlled swimming in semi-intact lampreys. Eur J Neurosci 12:4081–4092.

Sourkes TL, Poirier L (1965) Influence of the substantia nigra on the concentration of 5-hydroxytryptamine and dopamine of the striatum. Nature 207:202–203.

Stephenson-Jones M, Samuelsson E, Ericsson J, Robertson B, Grillner S (2011) Evolutionary conservation of the basal ganglia as a common vertebrate mechanism for action selection. Curr Biol 21:1081–1091.

Svensson E, Wikstrom MA, Hill RH, Grillner S (2003) Endogenous and exogenous dopamine presynaptically inhibits glutamatergic reticulospinal transmission via an action of D_2-receptors on N-type Ca^{2+} channels. Eur J Neurosci 17:447–454.

Thiele TR, Donovan JC, Baier H (2014) Descending control of swim posture by a midbrain nucleus in zebrafish. Neuron 83:679–691.

Vaaga CE, Borisovska M, Westbrook GL (2014) Dual-transmitter neurons: functional implications of co-release and co-transmission. Curr Opin Neurobiol 29:25–32.

van der Zouwen CI, Ryczko D (2020) Motor control: swim harder, faster, stronger. Curr Biol 30:R229–R232.

Villar-Cerviño V, Barreiro-Iglesias A, Mazan S, Rodicio MC, Anadón R (2011) Glutamatergic neuronal populations in the forebrain of the sea lamprey, Petromyzon marinus: An in situ hybridization and immunocytochemical study. Journal of Comparative Neurology 519:1712–1735.

von Twickel A, Kowatschew D, Saltürk M, Schauer M, Robertson B, Korsching S, Walkowiak W, Grillner S, Pérez-Fernández J (2019) Individual dopaminergic neurons of lamprey SNc/VTA project to both the striatum and optic tectum but restrict co-release of glutamate to striatum only. Curr Biol 29:677–685.e676.

Yoshida M, Tanaka M (1988) Existence of new dopaminergic terminal plexus in the rat spinal cord: assessment by immunohistochemistry using anti-dopamine serum. Neurosci Lett 94:5–9.